Atmospheric Research 318 (2025) 107998

Contents lists available at ScienceDirect

Atmospheric Research

journal homepage: www.elsevier.com/locate/atmosres

Impact of sudden stratospheric warming on tropospheric circulation and a cold wave formation: The case of the January 2019 event

O.N. Toptunova [a,b,*], M.A. Motsakov [a], A.V. Koval [a,b], T.S. Ermakova [a,b], K.A. Didenko [c]

[a] Russian State Hydrometeorological University, Saint-Petersburg, Russia
[b] Saint-Petersburg University, Saint Petersburg, Russia
[c] Pushkov Institute of Terrestrial Magnetism, Ionosphere and Radio Wave Propagation RAS, Moscow, Troitsk, Russia

ARTICLE INFO

Keywords:
Stratosphere-troposphere coupling
Cold wave
Stratospheric sudden warming
Tropopause folds
Isentropic analysis
Upper-level frontal zone

ABSTRACT

The present study is concerned with the aspects of stratosphere-troposphere dynamic interaction during major sudden stratospheric warming (SSW). The SSW observed in December 2018 – January 2019 was taken for consideration. The influence of the stratospheric polar vortex location on the position of the upper-level frontal zone (UFZ), changes in the steering flows in the middle troposphere, surface temperature anomalies, as well as on the characteristics of the tropopause have been studied using MERRA2 reanalysis data. Analysis has revealed that SSW events influence the location of the upper-level frontal zone (UFZ), subsequently altering steering flows in the troposphere and leading to the development of surface cold waves. Isentropic analysis have shown that SSW caused the intrusion of stratospheric air into the troposphere, which contributed to the intensification of the cold wave. Correlation analysis have demonstrated a statistically significant relationship between stratospheric processes and anomalies of geopotential height in the middle troposphere (500 hPa), exhibiting a two-week time lag following SSW events. Spatial distribution of the maximum correlation coefficient corresponds to the region with the UFZ deformation. In the cross-time interval of the formation of the SSW, 3-dimensional fluxes of planetary wave activity have been calculated. The enhanced reflection of wave activity over Canada during the SSW demonstrated the dynamic influence of the stratosphere on the troposphere, contributing to the formation of the cold wave.

This confirms the role of stratospheric-tropospheric coupling in surface weather extremes.

1. Introduction

Recently, due to the increasing requirements for long-range forecasting and climate models, there has been a growing interest in research of the stratosphere-troposphere interactions (Vargin et al., 2015) and, in particular, in studying the impact of stratospheric processes on the troposphere (Ayarzaguena et al., 2020; Baldwin et al., 2019). At the same time, as is known, the circulation, spatial and temporal scales in the troposphere and stratosphere differ, as well as the efficiency of the layers' influence on each other. The most striking stratosphere-troposphere couplings manifest as the event of sudden stratospheric warming (SSW) (Charlton and Polvani, 2007). Planetary waves (PW) generated in the troposphere by orography, the difference in the heating of continents and oceans, and baroclinic/barotropic instability propagate into the stratosphere, interact with the stratospheric polar vortex, contributing to the formation of SSW in the winter months. Variations of the stratospheric vortex affect the variability of the troposphere associated with the downward propagation of stratospheric anomalies through the reflection of PWs. With a decrease in altitude and an increase in atmospheric pressure, the reflected component of the wave weakens, as does its influence in the troposphere. Nevertheless, the structure and evolution of the stratospheric vortex can significantly affect surface anomalies (Mitchell et al., 2013; Nishii and Nakamura, 2005; Zhang et al., 2022).

SSW refers dynamic factors that form long-term anomalies in the troposphere. The polar vortex splits into two that move to lower latitudes, while subtropical anticyclones reach the pole during SSW events. In turn, the deformation of the polar vortex weakens the meridional temperature gradients between high and middle latitudes, which contributes to the penetration of cold air masses into the middle latitudes

* Corresponding author at: Russian State Hydrometeorological University, Saint-Petersburg, Russia.
E-mail addresses: olgakolp@yandex.ru (O.N. Toptunova), maxm@rshu.ru (M.A. Motsakov), a.v.koval@spbu.ru (A.V. Koval), taalika@mail.ru (T.S. Ermakova), didenko@izmiran.ru (K.A. Didenko).

https://doi.org/10.1016/j.atmosres.2025.107998
Received 16 October 2024; Received in revised form 15 February 2025; Accepted 16 February 2025
Available online 17 February 2025

and, as a consequence, the formation of cold waves at the surface (e.g., Thompson et al., 2002; Tomassini et al., 2012; Lehtonen and Karpechko, 2016). The dynamic aspects of SSW currently have been studied much better than their impact on weather conditions (White et al., 2019). This is explained by the nonlinearity and the multifactorial nature of the processes in the troposphere and different time responses in the stratosphere and troposphere. Hence, the latter is a promising research direction that will provide further insight into the features of stratosphere-troposphere coupling affecting the Earth's weather and climate, as well as improve the quality of long-range and seasonal forecasts of meteorological anomalies.

There are several theories describing the influence of stratospheric dynamics variability on the weather in the troposphere (Davini et al., 2014; White et al., 2019), but none of them can fully explain the mechanisms of this influence (Baldwin et al., 2019, 2021; Butler et al., 2019; Kidston et al., 2015; Tian et al., 2023). Pogoreltsev et al. (2020) considered the response of the tropospheric circulation to the SSW that occurred in January 2013 and 2014, and analyzed the synoptic consequences of the SSW. It was shown that surface Arctic anticyclones can be formed, subsequently moving over the territory of Eurasia southward and eastward, in particular towards China. Tomassini et al. (2012) showed that up to 40 % of extreme cold waves occur following disturbances recorded in the stratosphere. There is clear evidence from observations that the SSW is accompanied by the increased movement of air masses towards high latitudes in the troposphere, which causes surface pressure to rise in the Arctic (Baldwin et al., 2021). It has been shown that waves of both synoptic and planetary scales make a significant contribution to this process (Domeisen et al., 2013; Garfinkel et al., 2013; Hitchcock and Simpson, 2014; Smith and Scott, 2016; Simpson et al., 2009). At the same time, the tropospheric response to the SSW is confirmed not only by data analysis, but also by numerical experiments. Baldwin et al. (2021) suggested that temperature anomalies at high latitudes in the troposphere are associated with the movement of air masses towards the pole due to thermal spike in the stratosphere (i.e., SSW), and they enhance anticyclogenesis in the troposphere of high latitudes (Curry, 1987; Hoskins et al., 1985). Ding et al. (2023) suggested that sharp winter cooling and warming periods in the north of North America may be associated with periods of strengthening or weakening of wave activity in the stratosphere. They used the ERA5 reanalysis data and results of CMIP6 project. The SSW occurrence is connected with increased propagation of wave activity fluxes from the troposphere and the nonlinear interaction of PWs with each other and with the stratosphere zonal circulation (for example, Didenko et al., 2023), as well as with the sudden deformation of the polar vortex (Baldwin et al., 2021). Other studies also have revealed the consequences of SSW in the lower atmosphere in different regions of the Northern Hemisphere (e.g., Huang et al., 2021), including weather anomalies in Western Europe, the Far East and the eastern part of the North America (Garfinkel et al., 2017; Kolstad et al., 2010; Kretschmer et al., 2018; Lehtonen and Karpechko, 2016; Thompson et al., 2002). However, despite the results obtained, the coupling mechanisms between stratospheric dynamic processes and tropospheric circulation are still not fully understood, especially during such extreme events as SSW. To make an advance on this front, an understanding of the patterns in the propagation/reflection of PWs, the propagation of potential vorticity into the troposphere, and other dynamic processes during various types of SSW is required.

In this study the influence of the stratospheric polar vortex dynamics on the position of the upper-level frontal zone is studied, as well as the changes in the steering flows in the middle troposphere, surface temperature anomalies, and the tropopause variability during the major SSW event that occurred in winter 2018–2019. This SSW has previously been studied in detail both in terms of the stratospheric dynamic processes accompanying this event (Lee and Butler, 2020; Vargin et al., 2020) and in terms of the predictability of its occurrence and its impact on tropospheric dynamics (Rao et al., 2020). As was shown by Xu and Liang (2020), a large-scale cold air outbreak in the second half of January 2019 in North America occurred due to the amplification of planetary waves due to baroclinic instability caused by synchronization between zonal components of horizontal wind and temperature. However, what was the trigger for the emergence of this instability? Why did this particular configuration of dynamic processes arise in the region? We discuss these issues by conducting synoptic, correlation, isentropic, and wave activity analyses in the region. The study of stratosphere-troposphere coupling in this way may be important both from the point of view of long-range and seasonal forecasting of anomalies, and for more realistic modeling of climate change.

2. Methodology

To research dynamic atmospheric processes within the framework of this study, the MERRA2 reanalysis (Gelaro, et al., 2017) was used. Synoptic methods of analysis, isentropic approach and correlation analysis are applied. The zonal-mean temperature (at an altitude of 30 km between latitudes 77° and 87°N) and the zonal-mean zonal wind component (at an altitude of 40 km, 62.5°N) were used to determine the SSW time interval.

2.1. Synoptic methods of analysis

In accordance with the synoptic analysis of large-scale processes in a particular territory, without going into the weather of each day separately, for a general description of synoptic processes, it is appropriate to separate large-scale processes in the atmosphere in time and space. A natural synoptic region (NSR) is defined as a significant part of the hemisphere within which synoptic processes exhibit a certain degree of independence and can be studied separately from processes in other parts of the hemisphere. The NSR is characterized by a tropospheric pressure and temperature field that maintain a consistent pattern of synoptic development over several days. In the Northern Hemisphere, north of 30°N, three natural synoptic regions are identified: from Greenland to Taimyr Peninsula, from Taimyr Peninsula to the Bering Strait, and from the Bering Strait to Greenland. This division reflects the distribution of continents and oceans, which form differing heat and moisture fluxes. A natural synoptic period (NSP) represents the timeframe during which a specific synoptic process unfolds over an NSR; that is, a consistent pressure and temperature fields maintain a particular orientation of surface pressure system movement and the geographical location of their centers within the NSR. Transitions between NSPs are marked by rapid restructuring of the tropospheric pressure and temperature fields, leading to a new orientation of pressure system movement and a shift in the location of their centers. The duration of an NSP ranges from 3 to 10 days, averaging around 6–7 days. This principle can be applied as one of techniques in long-term forecasting (Vil'fand et al., 2017).

The upper-level frontal zone (UFZ) position changing is one of markers showing the beginning of a new NSP over the natural synoptic region. Surface temperature and pressure anomalies were preliminarily calculated relative to the average value of 1980–2022, and periods of conditionally homogeneous circulation within NSRs and NSPs were established for the troposphere analysis. The position of the UFZ for a given synoptic region was established on each of the days of the conditionally homogeneous circulation period. The position of the UFZ was determined by the closely spaced isolines at 500 hPa geopotential height, since in its essence the UFZ is a transition zone between high-level cold cyclones and high-level warm anticyclones in the middle and upper troposphere. The position of the UFZ determines the movement of various air masses. Thus, when it shifts to the South, colder Arctic air masses penetrate southwards, accomplishing polar and ultrapolar invasions. This is often accompanied by the formation of tropopause folds, which contribute to the penetration of stratospheric air deep into the troposphere. Baldwin et al. (2024) demonstrated that

the strength of the stratospheric polar vortex is related to the height of the polar tropopause, engendering polar tropospheric air stretching/compression. The steering flows determining the movement and temperature-humidity characteristics of air masses were specified at 500 hPa geopotential height. Surface temperature anomalies were calculated as the difference between the temperature value at each node and its climatic value.

2.2. Correlation analysis

Geopotential anomalies were calculated at 500 and 7 hPa levels, followed by a correlation analysis with a shift to study the stratospheric influence on the troposphere. The 7 hPa level was fixed and all the underlying levels shifted by a day. The value of geopotential anomalies in each grid node was correlated. In total, the shift was calculated for 30 days. The significance of the correlation coefficient was estimated by Fisher's F-statistics at a 5 % significance level. Usually, for the analysis of SSWs, it is essential to use a height of 10 hPa (Charlton and Polvani, 2007), however, in many cases it is more convenient to choose a height of 7 hPa, because there are a number of SSWs that were not accompanied by deep downward penetration and a reversal of the zonal wind at 10 hPa, while the temperature anomalies and their influence on the extratropical circulation were comparable with canonical major SSWs (Kozubek et al., 2020; Savenkova et al., 2017).

2.3. Isentropic analysis

The influence of the stratosphere on the troposphere is efficiently analyzed by considering vortex and/or geopotential anomalies. Vortex anomalies are not very convenient for analysis, since this characteristic is quite variable and, accordingly, noisy. However, the transfer of vorticity can be traced in an isentropic coordinate system. An isentropic surface is a surface with an equal potential temperature. Since dry-adiabatic processes occur on one isentropic level, this makes them a more reliable tool for analysis than pressure levels, since the movement of air parcels can be traced on them in more detail. This approach makes the analysis three-dimensional, allowing the analysis of vertical flows. In the middle and upper troposphere, the potential vorticity anomaly values range from 0.5 to 1.5 10^{-6} m^2 K/s kg. According to WMO, the dynamic tropopause level is 1.6 10^{-6} m^2 K/s kg (WMO, 1986). The most common threshold value for the dynamic tropopause is the surface at which the potential vorticity values are 2.0 10^{-6} m^2 K/s kg (Škerlak et al., 2015; Akritidis et al., 2016; Holton et al., 1995), although some researchers point out that a level of 3.5 10^{-6} m^2 K/s is a more adequate reflection of the tropopause position (Hoerling et al., 1991; Kunz et al., 2011), since it is in better agreement with the thermal tropopause. The tropopause level can be determined at the isentropic level of 310 K (Woiwode et al., 2018; Kunz et al., 2011). In the isentropic representation, there is no difference between the tropopause of low and high latitudes (which in the traditional representation have different heights and are therefore inconvenient for analysis). Isentropic levels can be approximately considered as material ones, since the isentropic levels can vary in height (z) and pressure (p), the horizontal flow along the surface includes the adiabatic component of the vertical displacements dz/dt and dp/dt, which would otherwise be obtained as a separate velocity component in Cartesian or isobaric coordinates. This factor allows more accurate tracking of the trajectories of individual air parcels with similar thermodynamic properties. Isentropic analysis within the context of the current study can be interpreted as approach to studying the interaction of the stratosphere and troposphere, as far as it shows the penetration of stratospheric air into the troposphere occurring after the SSW onset and the formation of tropopause folds.

2.4. Planetary wave activity

To demonstrate the two-way vertical troposphere-stratosphere coupling, a 3-dimensional wave activity flux of planetary waves is used, calculated using the approach proposed by Plumb (1985). This approach involves calculating the direction of propagation of the wave momentum flux in a three-dimensional coordinate system and has been successfully used in studying the vertical propagation of waves from the stratosphere to the troposphere (e.g., Zyulyaeva and Zhadin, 2009; Wei et al., 2021) and their reflection in the opposite direction (see, e.g., Vargin et al., 2022). Plumb's three-dimensional wave activity flux is convenient because it allows analyzing the dynamic interaction of the stratosphere and troposphere at the regional level (Wei et al., 2021; Gečaitė, 2021).

3. Results

3.1. The SSW event and the prerequisites for its formation

In the current study we observe the SSW event that began to form at the end of December 2018, reaching its maximum around January 1, 2019 (see Fig. 1 for temperature rise moment).

In the equatorial stratosphere, at 50 hPa, the easterly phase of the quasi-biennial oscillation (QBO) of the equatorial zonal wind was observed (https://acd-ext.gsfc.nasa.gov/Data_services/met/qbo/qbo.html), which in turn contributed to the increase in the activity of PWs, according to Holton-Tan mechanism (Holton and Tan, 1980; Anstey et al., 2022). In particular, on the eve of the SSW, a simultaneous increase in PW1 and PW2 (planetary waves with zonal wave numbers 1 and 2, respectively) was observed (Fig. 1b, c): the first one intensified throughout December, and the second one intensified in the second decade of December. This led to a very powerful stratospheric event. At altitudes from 40 to 60 km, the increase in PW1 occurred in the first two decades of December, which also caused the deepening of the polar vortex in the corresponding time intervals.

Figure 2 shows the geopotential anomalies calculated based on the MERRA2 reanalysis (the mean value was calculated from 1980 to 2022), averaged over decades in December.

In the first two decades (Fig. 2a and b), the polar vortex deepens (simultaneously with the strengthening of PW1), but in the third decade, it intensively weakens, which is not typical for this time of year, as indicated by high positive anomalies in Fig. 2c. In the third decade, prerequisites for SSW were formed. With a sharp weakening of the PW1 amplitude, the vortex became unstable, and then it displaced by the anticyclone and the direction of the zonal wind changed. The maximum increase in temperature and strengthening of the easterly wind are noted on January 2 (Fig. 3), along with the splitting of the vortex into separate cells.

The SSW duration was approximately 3 weeks, with 1 week of temperature increase and zonal wind reversal, and 2 weeks of the stratosphere returning to the usual state. Such warming, according to the WMO definition, has to be classified as major. It caused a fairly strong response in tropospheric processes, discussed further.

3.2. The SSW influence on the position of the UFZ

Now we consider the influence of the stratospheric vortex position on tropospheric processes, in particular, on the position of the planetary UFZ. Any forecast begins with an assessment of macrosynoptic objects, and therefore the analysis of the synoptic position for a short-term and medium-term weather forecast begins with determining the position of the planetary UFZ. The expected position of the UFZ, its type and shape, is one of the methods of long-term forecasting. The position of the UFZ determines the areas where the formation of new pressure systems, is most likely.

The formation of UFZ occurs under the influence of two factors: thermal and dynamic. The thermal factor is due to the different radiation balance of latitudinal zones and, as a consequence, a significant temperature gradient. The dynamic factor is due to the movement of

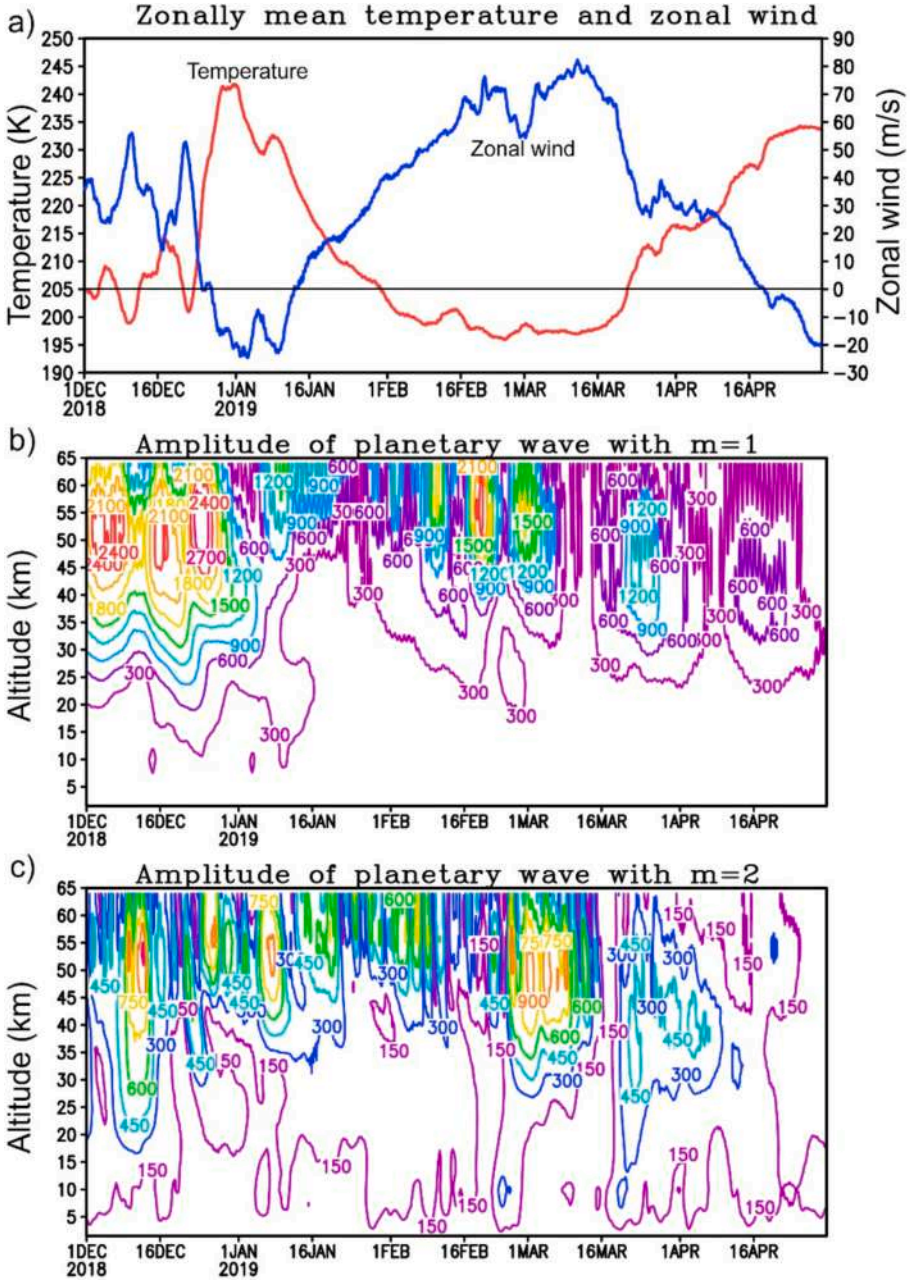

Fig. 1. a) Zonal-mean temperature at 30 km, 77°-87°N (red line) and zonal-mean zonal wind component at 40 km, 62.5° N (blue line); b) amplitude of PW with zonal number 1 in the field of geopotential height; c) amplitude of PW with zonal number 2 in the field of geopotential height. (For interpretation of the references to color in this figure legend, the reader is referred to the web version of this article.)

planetary Rossby waves in the troposphere, forming upper-level troughs and ridges. In the general westerly transfer, these waves move, and zonal distribution of troughs occurs. The heterogeneity and non-stationarity of such movement creates areas with different spacing of isolines (closely and widely spaced). Due to the influence of dynamic factors, the Rossby wave loses stability in some region, and the wave amplitude increases. At the same time, the general zonality of processes in this area is disrupted, and a meridional circulation shape is formed. Usually, on a spatial scale, such an influence is limited by the boundaries of natural synoptic regions. The division of the territory into NSRs, where a certain type of synoptic processes is preserved for a long time, is usually carried out in long-term forecasting. In recent studies (Didenko et al., 2024), it was confirmed that the response in different sectors of the Northern Hemisphere to ongoing stratospheric events is not the same and it is possible to divide the area of the Northern Hemisphere into longitudinal sectors. According to Didenko et al. (2024), the most active response in the troposphere was over the territory of Canada, which the authors attributed to the separate sector (or NSR). In this region, which the authors included Canada, Greenland, the United States, and the North Atlantic, the maximum downward wave activity flux is observed for the months from December to March based on the results of averaging for 10 years (2008–2017).

The stratospheric polar vortex is stretched throughout January (Fig. 4a,b), its center is shifted towards Canada. Later, a separate center is formed over Siberia (Fig. 4c), but its influence will not affect the UFZ, since at this time the weather at the surface is determined by a powerful Siberian anticyclone (i.e. the thermal factor prevails here, and the UFZ passes to the South).

Let us consider the features of the tropospheric circulation at the level of 500 hPa and its changes during natural synoptic periods. NSPs

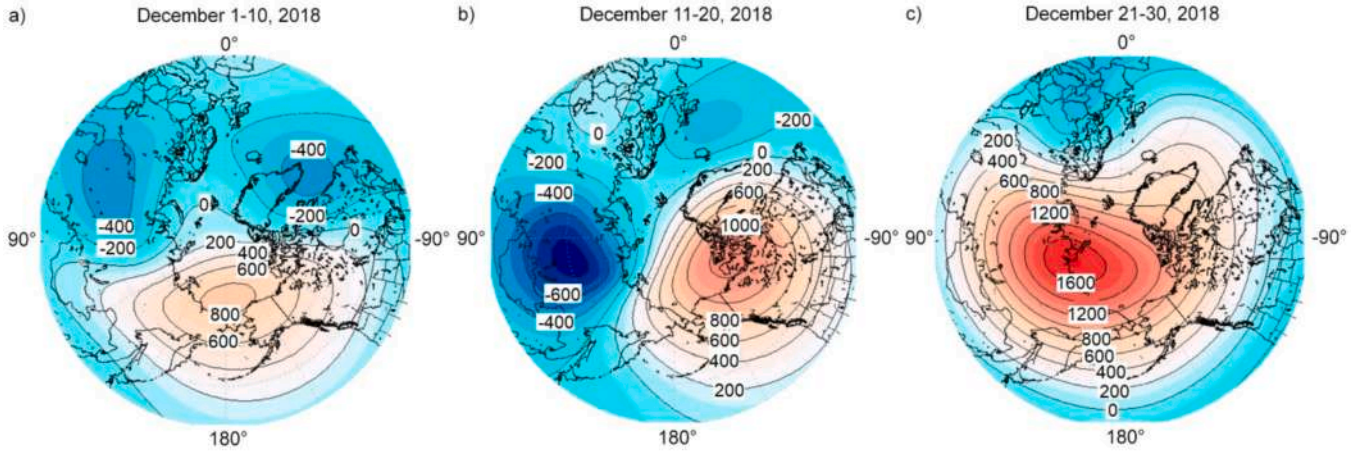

Fig. 2. Decade-by-decade geopotential anomalies at a height of 7 hPa (gpm): a) 1–10 December; b) 11–20 December; c) 21–20 December.

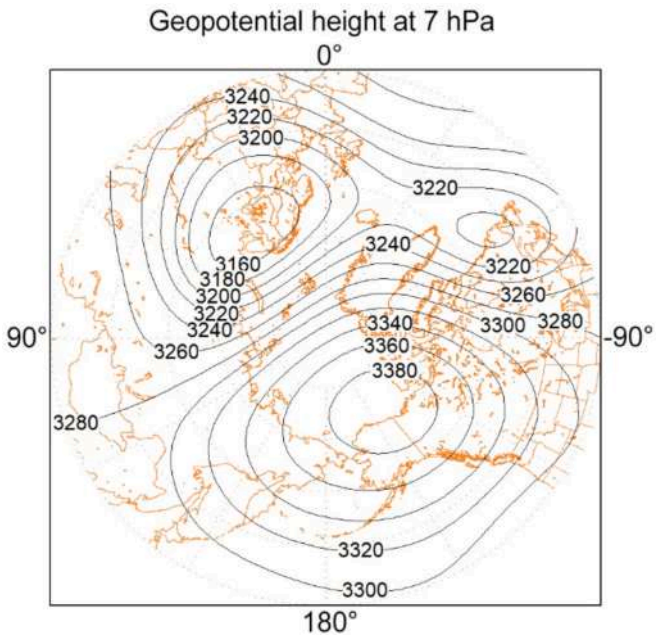

Fig. 3. Polar vortex on January 2nd, 2019 at an altitude of 7 hPa: the contours show the geopotential height (×10 gpm).

were identified based on synoptic analysis of surface temperature and pressure anomalies. One of the symptoms of the natural synoptic period change is a change in the position of the UFZ. The spaghetti charts were prepared for the isoline of axial 552 gpdam for similar periods (see Fig. 5). This certain value was identified using the synoptic method based on the analysis of 500 hPa geopotential fields. Fig. 5a-c show the daily position of the 552 gpdam isoline (color is a separate day within the natural synoptic period). It is shown that the zonal circulation, characteristic of the first period (Fig. 5a), is gradually disrupted, the trough over eastern Canada deepens, and the ridge over the west coast intensifies after the SSW, on January 8–15 (Fig. 5b). A significant distortion of the UFZ occurs (Fig. 5b) with weakening of oscillations by the end of the period (Fig. 5c) (the periods are distinguished here by the conditionally homogeneous circulation in the lower and middle troposphere for this region). The peculiarity of division into NSPs implies that within its framework the position of the UFZ is quasi-stationary. This position of the UFZ facilitates the penetration of colder air masses from the pole into central and eastern Canada. It should be noted that the deformation of the UFZ during January in Fig. 5 is observed only over America; in other longitudinal sectors, deformation does not occur, i.e. the isolines shown in Fig. 5 are quasi-parallel to the latitudinal circle at other longitudes.

In order to show that the change in the UFZ occurred not after the SSW event, but as a result of this event, a correlation analysis of the geopotential anomaly fields was made. As is known, the troposphere affects the stratosphere mostly through the upward propagating planetary waves, in turn, the reverse effect is manifested through a change in

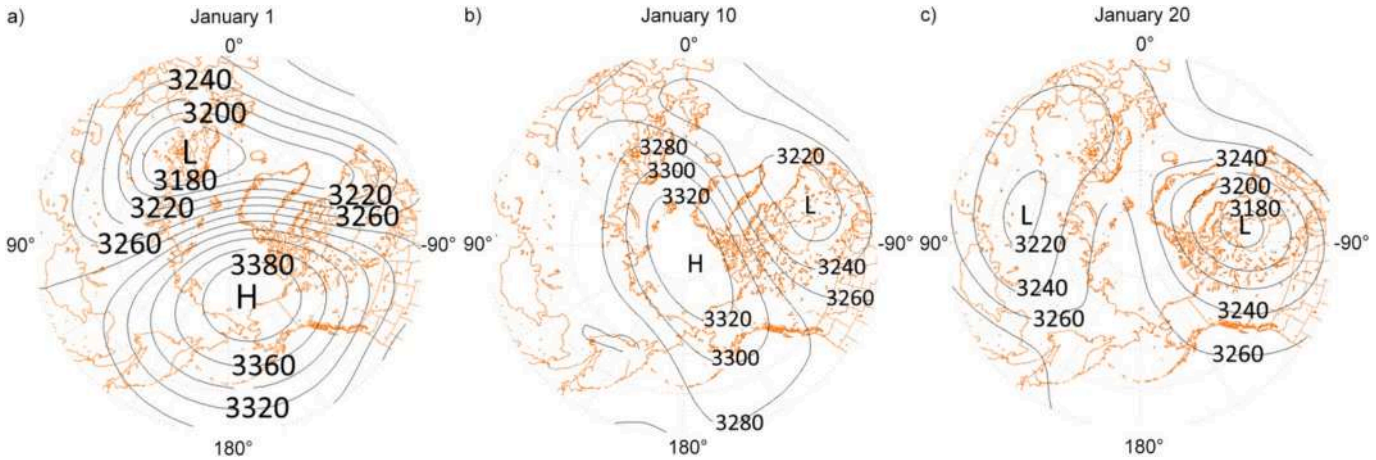

Fig. 4. Stratospheric polar vortex position in the field of geopotential height at 7 hPa level (×10 gpm): a) on January 1st; b) on January 10th; c) on January 20th.

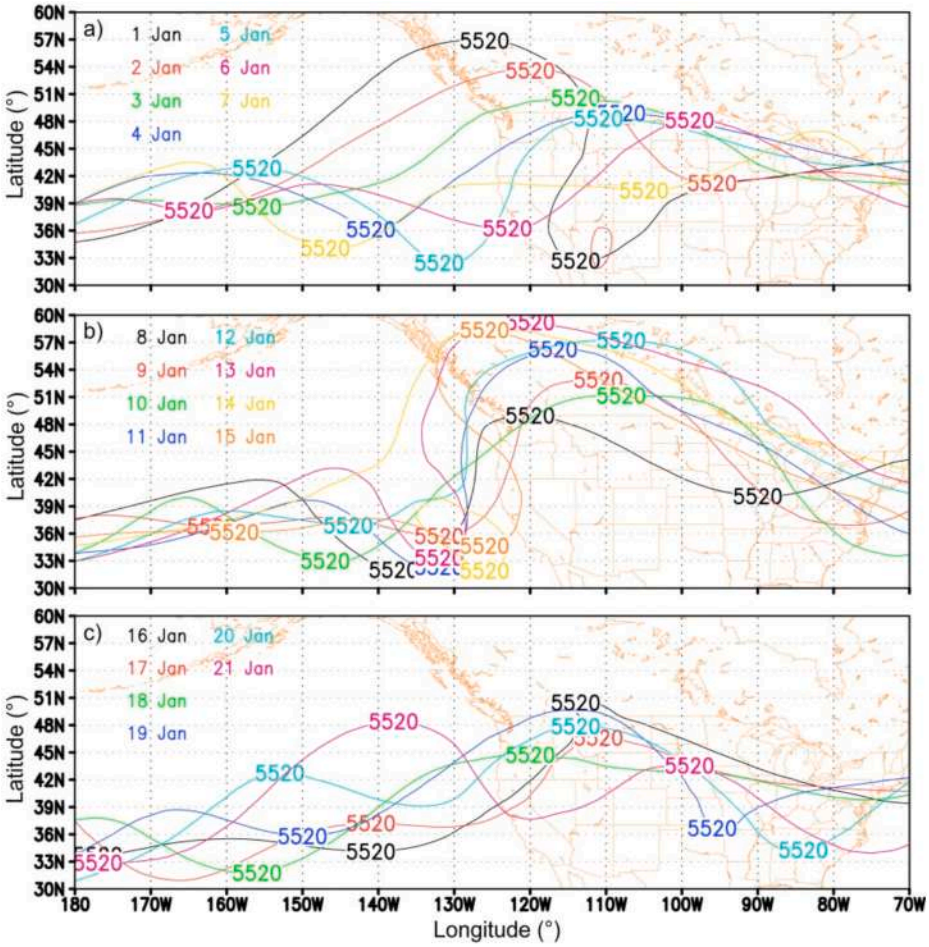

Fig. 5. Position of the upper-level frontal zone (500 hPa level) defined within the natural synoptic period in January: a) 1–7 January; b) 8–15 January; c) 16–21 January.

tropospheric circulation. This change causes a violation of the stability and breaking of the Rossby wave, and as a consequence, a change in the steering flows, that is, it is manifested through geopotential anomalies. To study the influence of the stratosphere on the troposphere, a correlation analysis with a shift was used. Despite the fact that the variability of the geopotential is manifested not only in time and height, but also in space, such a tool can be used for a fairly rough estimate of the changes that occur, especially considering that the variability in the middle troposphere (Fig. 6a) is not as high as in the stratosphere (Fig. 6b). Thus, the standard deviation for the 500 hPa level for January is within 200 gpdam (see Fig. 6a).

3.3. *Vertical coupling between troposphere and stratosphere after the SSW*

One of this study objectives was to find a connection between the anomalies of 500 hPa and 7 hPa. The choice of the 500 hPa level is due to the fact that this is the middle troposphere, which determines the

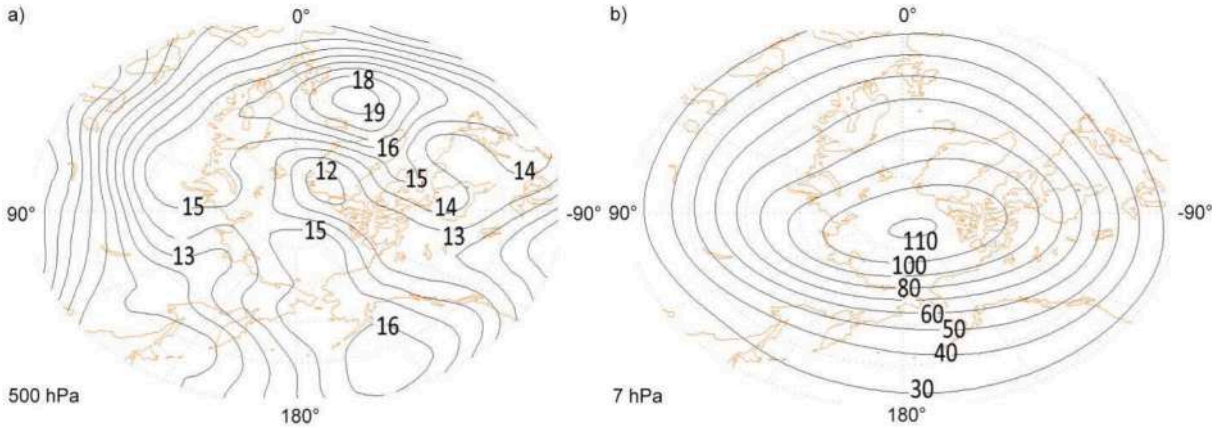

Fig. 6. Standard deviation of a) 500 hPa geopotential height; b) 7 hPa geopotential height for January (relative to the mean value of 1980–2022) (×10 gpm).

transfer of lows and highs. This level is important for the determination of the steering flows' direction in synoptic practice. The 7 hPa level was fixed, and the data at the 500 hPa level were shifted in time. The value of the geopotential anomalies in each grid node was correlated. In total, the shift was calculated for 30 days And the significance of the correlation coefficient was estimated as it was described in section 2.

Figure 7 shows only significant correlation coefficients on the day when the temperature was maximum, (we designate this as the central date, Fig. 7a) as well as with a shift of 10, 15, 20, 25 and 30 days (Fig. 7b-f, respectively). As can be seen, on the day of the central date (Fig. 7a), the stratosphere and the troposphere are weakly interact, since the time response of the signal here is different, but after two weeks the signal from the stratosphere penetrates and the correlation coefficient increases in magnitude. It can be noted that this coefficient is maximum in magnitude (Fig. 7c) in the region where the UFZ changed (curvature of isolines changed). The shift of the stratospheric vortex leads to an increase in the high-altitude ridge in the region of Canada at a height of 500 hPa, as indicated by the negative correlation coefficients. Since 500 hPa level is usually associated with the steering flows in the troposphere, it can be concluded that the stratosphere affects the shift of surface pressure changes through a change in the UFZ. The SSW event disrupted the zonal circulation.

After specifying the UFZ position within the NSP, temperature and geopotential anomalies were calculated for the same period. Fig. 8a-c shows the geopotential height anomalies (shading) and their absolute values (contours), averaged over the selected natural synoptic periods. A strong ridge over the Atlantic is noted at 500 hPa level, which gradually weakens by the end of the period. The consequence of the SSW is the strengthening of the ridge over the Alaska – western Canada, which is not typical for this period, as indicated by the positive anomalies. The shift of the upper-level center of cyclone (at 7 hPa) occurs in this region, as a result of which an upper-level ridge is formed here, as indicated by significant negative correlation coefficients. Accordingly, the steering flows become more meridional ones and cold Arctic air masses rush to lower latitudes of the continent. Similar trends in polar pressure increase during SSW events were previously discussed by Baldwin et al. (2021), who processed data on 36 SSW events from 1958 to 2015 obtained from the Japanese 55-year reanalysis (JRA-55). In particular, they demonstrated an enhancement of meridional tropospheric flows contributing to this effect.

In turn, the restructuring of macrofields in the middle troposphere affected the direction of the steering flows and the trajectory of lows and highs. Fig. 8d-f show temperature anomalies reflecting the increasing cold wave that occurred due to the shift of the steering flows over Canada to the northwest, i.e. the region became subject to the influence of the cold Arctic air mass.

To demonstrate the changes in the vertical stratosphere-troposphere interaction in the vicinity of the SSW, we constructed the latitude-height distributions of the anomalies of the 3-D Plumb wave activity flux (see Section 2) relative to the 10-year average values. December 25, shown in Fig. 9a, corresponds to the maximum strengthening of the planetary wave in the first phase of the SSW shown in Fig. 1b. Fig. 9b and c correspond to the maximum increase in stratospheric temperature on January 1 and 3. January 10 in Fig. 9d corresponds to the weakening of wave activity and the continuation of the formation of the cold wave in Canada. The calculated standard deviation of the vertical component of the wave activity flux over 10 years is of order of 0.2 in most of the distributions in Fig. 9, which indicates the statistical significance of the presented anomalies. In December 25 in Fig. 9a, positive anomalies of the Plumb vertical component predominate, indicating an increase in the propagation of wave activity from the troposphere to the stratosphere poleward from 50° N against the background of a general

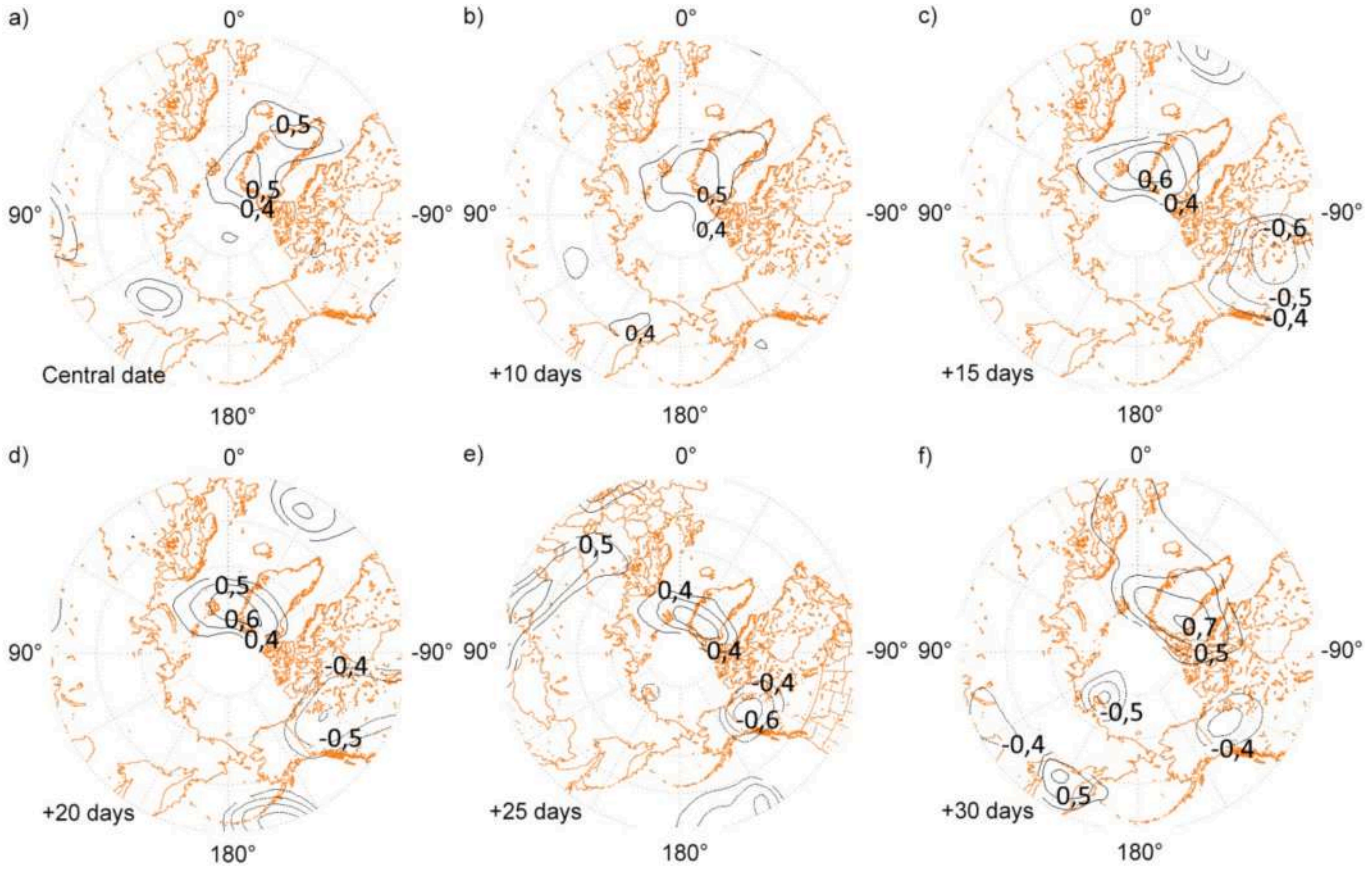

Fig. 7. Significant correlation coefficients between 7 hPa and 500 hPa geopotential anomalies a) on the central date; b) with a shift of 10, 15, 20, 25 and 30 days (b-f, respectively).

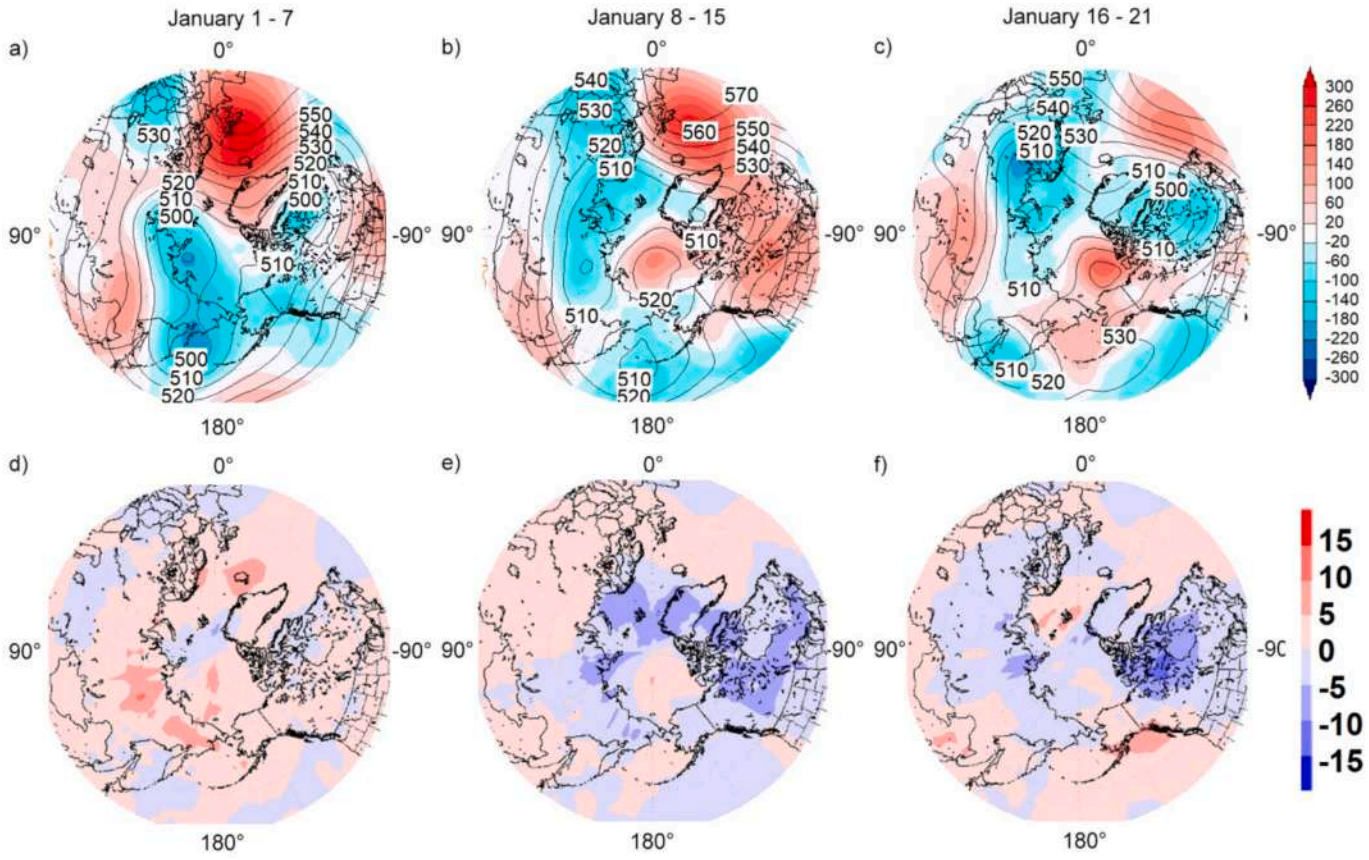

Fig. 8. 500 hPa geopotential anomalies (color coding) and absolute values of 500 hPa geopotential (×10 gpm, contours) for a) 1–7 January; b) 8–15 January; and c) 16–21 January; corresponding anomalies of the surface temperature for the same time intervals.

increase in wave activity in the first phase of the SSW. However, during the SSW peak, between January 1 and 3, a strong reflection of the planetary wave is observed, which contributes to the direct dynamic effect of the upper layers of the atmosphere on the lower ones during the SSW peak (see, e.g., Perlwitz and Harnik, 2004; Vargin et al., 2022). After the SSW, the wave activity anomalies decrease, bringing the distribution closer to the climatic norm. However, the process of momentum transfer from the reflected waves around the SSW peak already contributed to the deformation of the UFZ and the beginning of the cold invasion into the troposphere in the Canadian sector, discussed below.

To further study the dynamic vertical interaction of the troposphere with the stratosphere after the SSW and to analyze the relationship of the SSW with the onset of the cold wave in America, we turn to the spatial distribution of the 3M vortex. Fig. 10 shows isentropic maps of potential vorticity and wind at a level of 310 K (top panels), daily anomalies of surface temperature (middle panels), and vertical sections of the Ertel vortex in the isentropic coordinate system for a latitude of 62 N (bottom panels). The data in Fig. 10 are presented in the vicinity of the SSW maximum (January 1 and 3 - a and b, respectively). If there is no advective change in temperature, the value of the potential vorticity (PV) on the isentropic surface remains unchanged. High PV values determine a low tropopause and a cold air mass. The bottom Fig. 10a shows that on January 1, PV increases over eastern Canada, and at the same time, the ground cold wave also increases (middle Fig. 10a). Then, the temperature anomalies in the region under consideration increase, PV increases even more, and by January 3, a tropopause fold is formed here: a closed isobar of 325 hPa in the top Fig. 10b. Then, on January 3, PVU values greater than $6 \bullet 10^{-6}$ ($m^2 \bullet K/s \bullet kg$) descend into the middle troposphere, below 7.5 km, indicating the penetration of stratospheric air into the troposphere.

Then high PV values spread to the entire north of the continent and by January 10 the tropopause fold is already formed over Alaska (see Fig. 11a). Fig. 11 shows the same data as Fig. 10, but for January 10 and 17 (a and b, respectively), except that the vertical sections of the Ertel vortex in the lower panels of Fig. 11 are shown at 66 N. Unlike Fig. 10, a different latitude was chosen here so that the section would pass through the tropopause fold.

The further development of the cold wave in the second ten-day period of January (Fig. 11) may be due to the mechanism described below. As described by Moore (1993), vertical movements in the isentropic coordinate system are described by the equation:

$$\omega_\theta = \frac{dp}{dt} = \left(\frac{\partial p}{\partial t}\right)_\theta + \vec{V}^* \nabla_\theta p + \frac{\partial p}{\partial \Theta}\frac{d\Theta}{dt} \quad (1)$$

where ω_θ is the analogue of vertical velocity in the isentropic coordinate system; p is pressure; Θ is the potential temperature $\Theta = T\left(\frac{1000}{P}\right)^{\frac{R_d}{C_p}}$. The second term on the right-hand side of (1), describing horizontal pressure advection on an isentropic surface, is written as:

$$\vec{V}^* \nabla_\theta p = u\left(\frac{\partial p}{\partial x}\right)_\theta + \nu\left(\frac{\partial p}{\partial y}\right)_\theta \quad (2)$$

Here u and ν are the zonal and meridional components of the wind. However, from the definition of potential temperature, it follows that on surfaces of equal potential temperature, isobars can be considered as isotherms. From the equation of state of an ideal gas $P = \rho RT$ and the definition of potential temperature, it follows that on isentropic surfaces, lines of equal pressure can also be considered as lines of equal density. Thus, according to Moore (1993), on isentropic surfaces, pressure advection can be considered as temperature advection. That is, if on an isentropic surface the wind blows from a high-pressure area to a low-

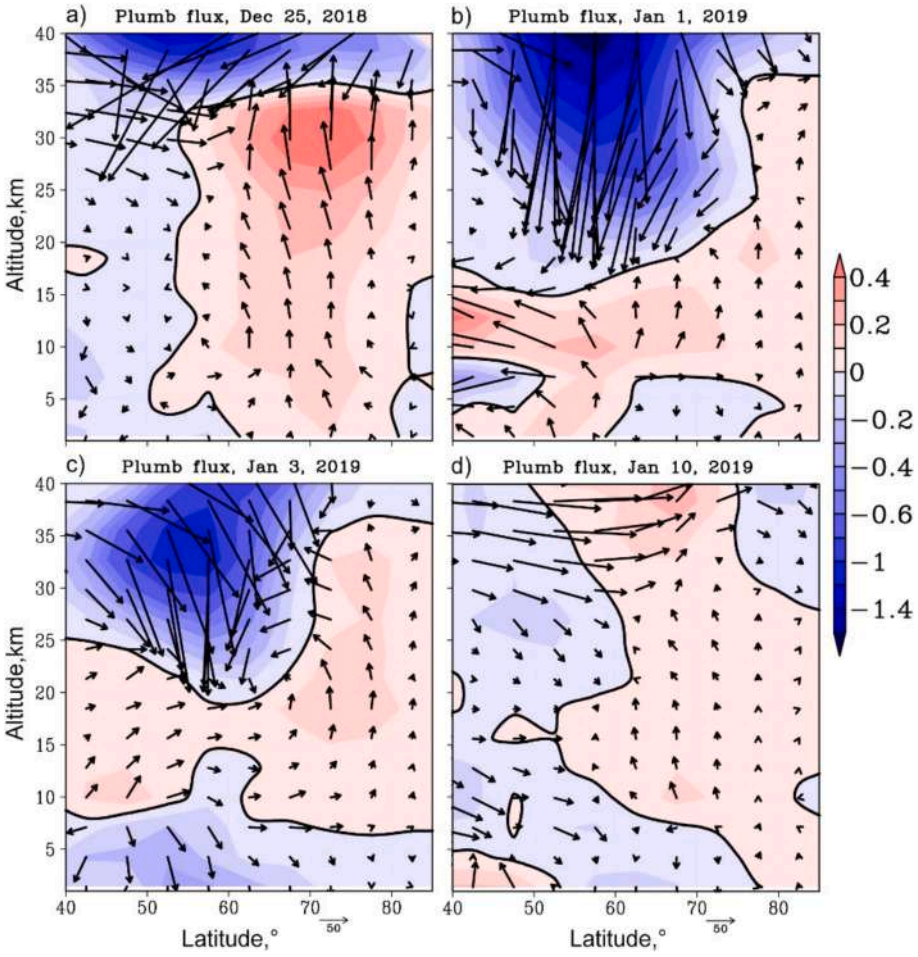

Fig. 9. Latitude-height distributions of 3d wave activity flux (arrows, m^2/s^2) anomaly relative to climate values (2010–2019) averaged over longitudes of 60°W-170°W for December 25 (2018), January 1, 3, 10 (a-d, respectively), shaded areas show anomaly of the vertical flux component.

pressure area, then air rises forming heat advection. If on an isentropic surface the wind blows from a low-pressure area to a high-pressure area, then air sinks forming cold advection.

Now we consider the processes of the second ten-day period of January. After January 10, no significant changes in the Ertel vortex field on the isentropic surface of 310 K (approximately the height of the dynamic tropopause) are observed, but the wind field at 310 K in the upper panels of Fig. 11 reflects a change in the nature of advection. Thus, if we consider the pressure field as a temperature field according to Moore (1993), then cold advection occurs in the north of Canada, while a fairly high PV value remains here. At the border with Alaska, as well as in Alaska itself, heat advection occurs. By the end of the first ten-day period of January, the cold wave intensifies. On the isentropic maps (January 17), over the center of the continent, the wind blows from the area of low pressure (temperatures) to the area of high pressure. The temperature here decreases. In the east of the continent, the reverse process (from high to low) occurs, which would contribute to an increase in temperature, expressed in this case in a weakening of the cold wave. Over Alaska, the flows also already cause heat advection.

In terms of the SSW impact on tropospheric circulation, according to the model studies of Gerber et al. (2009) and Hitchcock and Simpson (2014), it is determined primarily by tropospheric variability. The presence of direct forcing from above, such as planetary wave reflection, tropopause folds, and stratospheric air invasion into the troposphere, should be combined with a stochastic component associated with internal tropospheric variability. This should enhance the SSW signal below, and in our case, it manifests itself in the UFZ deformation and the formation of the horizontal pressure advection demonstrated above. As a result, the processes under consideration lead to the establishment of a quasi-stationary wave structure that accompanied the intensification of the cold wave in America in the second half of January (Xu and Liang, 2020).

4. Summary and conclusion

In this study using the case of the major SSW event observed in December 2018 – January 2019 the features of stratosphere-troposphere interaction are investigated. Using the MERRA2 reanalysis data the influence of the stratospheric polar vortex location on the position of the upper-level frontal zone (UFZ), changes in the steering flows in the middle troposphere, surface temperature anomalies, as well as on the tropopause characteristics is studied. To investigate large-scale dynamics the basic principles of analysis used in long-term forecasting by synoptic methods, methods of the isentropic approach, as well as correlation analysis and planetary waves activity analysis are applied. Key findings are as follows:

- The result of the SSW was a change in the UFZ shape with a subsequent change in the direction of the steering flows over the Canada. The UFZ deformation (the trajectories of pressure systems are associated with UFZ) occurred approximately 15–20 days after the SSW central date (maximum stratospheric temperature). The steering flows in the UFZ deformation zone intensified in the meridional direction, and the zonal transfer in the middle troposphere was restored after another 10 days. The steering flows change caused the formation of a cold wave over Canada.

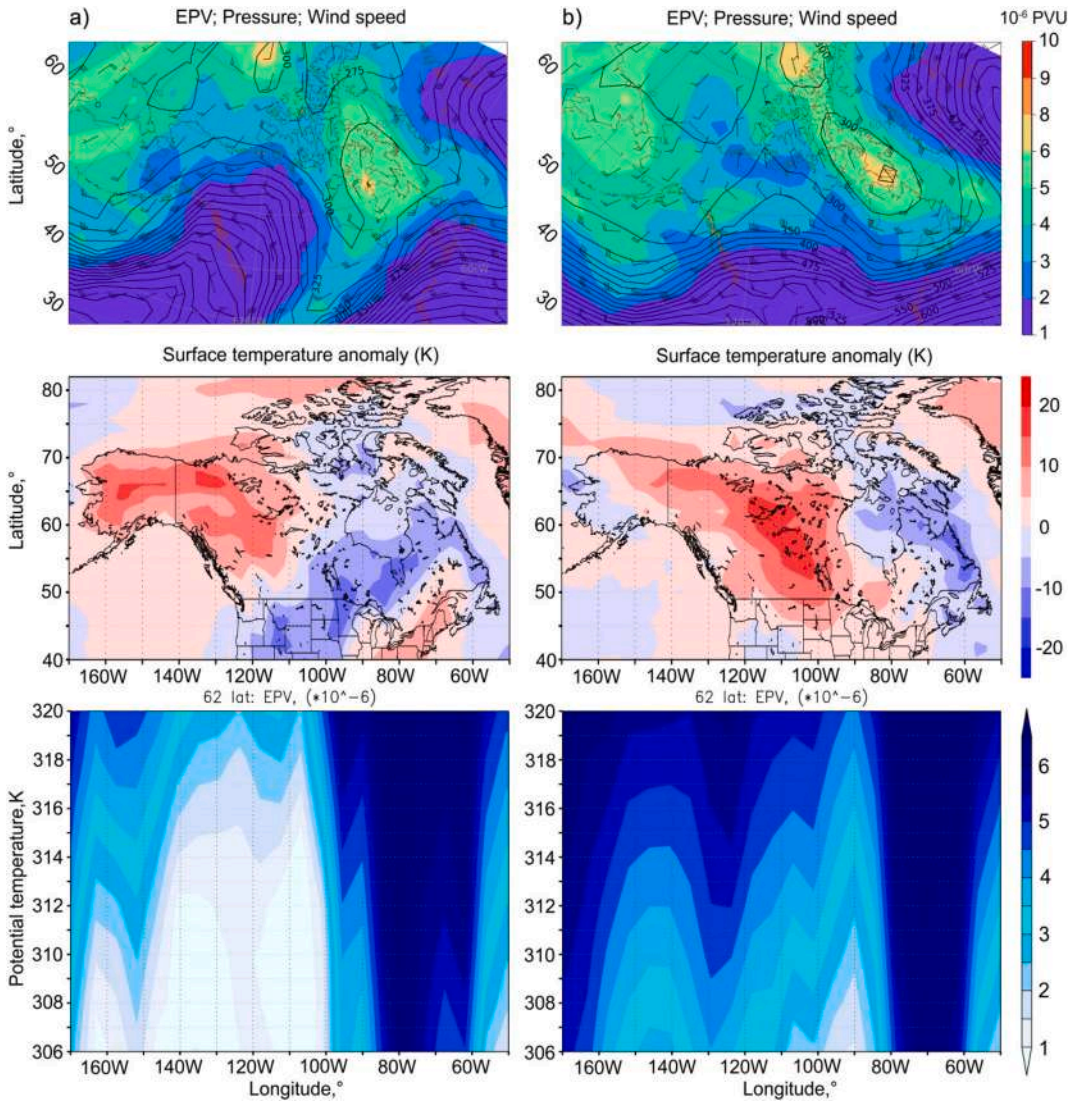

Fig. 10. Ertel's potential vortex, pressure and wind on the 310 K isentropic surface (top row); daily surface temperature anomaly (middle row), both, for the region 60°W-170°W and 40°N-90°N; vertical cross-section of the Ertel vortex field at 60°W-170°W, 62°N (bottom) on January 1st and 3rd (a, b, respectively).

- Isentropic analysis showed that, in addition to the flows' change in the middle troposphere, the SSW caused the intrusion of stratospheric air into the troposphere, which, in turn, further intensified the onset of the cold wave. Such an intrusion of air from the stratosphere with a high vorticity value contributed to a general decrease in the tropopause height and the formation of tropopause folds. Accordingly, the tropopause height decreases with the downward movement of the air flow with a high value of potential vorticity.
- Correlation analysis with a time shift was used to study the influence of the stratosphere on the troposphere. The aim of the study was to find a connection between geopotential anomalies at 500 hPa and anomalies at 7 hPa. Starting with a time lag of 2 weeks the correlation of geopotential variation at these levels is observed, whereas the maximum correlation coefficient corresponds to the region with the UFZ deformation. The displacement of the stratospheric vortex leads to ridge intensification in the Canadian region at 500 hPa. Since this level is usually associated with the steering flows in the troposphere, it can be concluded that the disturbances of the stratosphere associated with the SSW affect the displacement of pressure systems.
- Analysis of 3-dimensional wave activity fluxes showed an intensification of the descending branch of the flux during the SSW over the Canadian sector, which confirms an increase in the dynamic impact of the stratosphere on the troposphere, contributing to the establishment of a quasi-stationary wave structure that accompanied the intensification of the cold wave in America in the second half of January.

Despite its strength and long persistence in the stratosphere, SSW in January 2019 doesn't refer to classic “downward propagating” event according to criteria proposed by Karpechko et al. (2017). In the time interval of the SSW formation and after the event, vertical stratosphere-troposphere coupling was relatively weak. Downward translation of the SSW signal stopped at tropopause (Lee and Butler, 2020; Butler et al., 2020). However, it was precisely this signal, as we were able to show, coupled with the increased reflection of wave activity, that was sufficient to form the tropopause folds and to deform the steering flows over Canada, which facilitated the penetration of cold air deep into the troposphere.

The present work study of the features of vertical interactions of the stratosphere with the troposphere during the formation of such extreme external influences as SSW is important for understanding the processes, which must be taken into account in the long-range forecasting, including sub-seasonal to seasonal (S2S) forecasting (Vitart and Anderson, 2012). The statistics of such phenomena during SSW of various

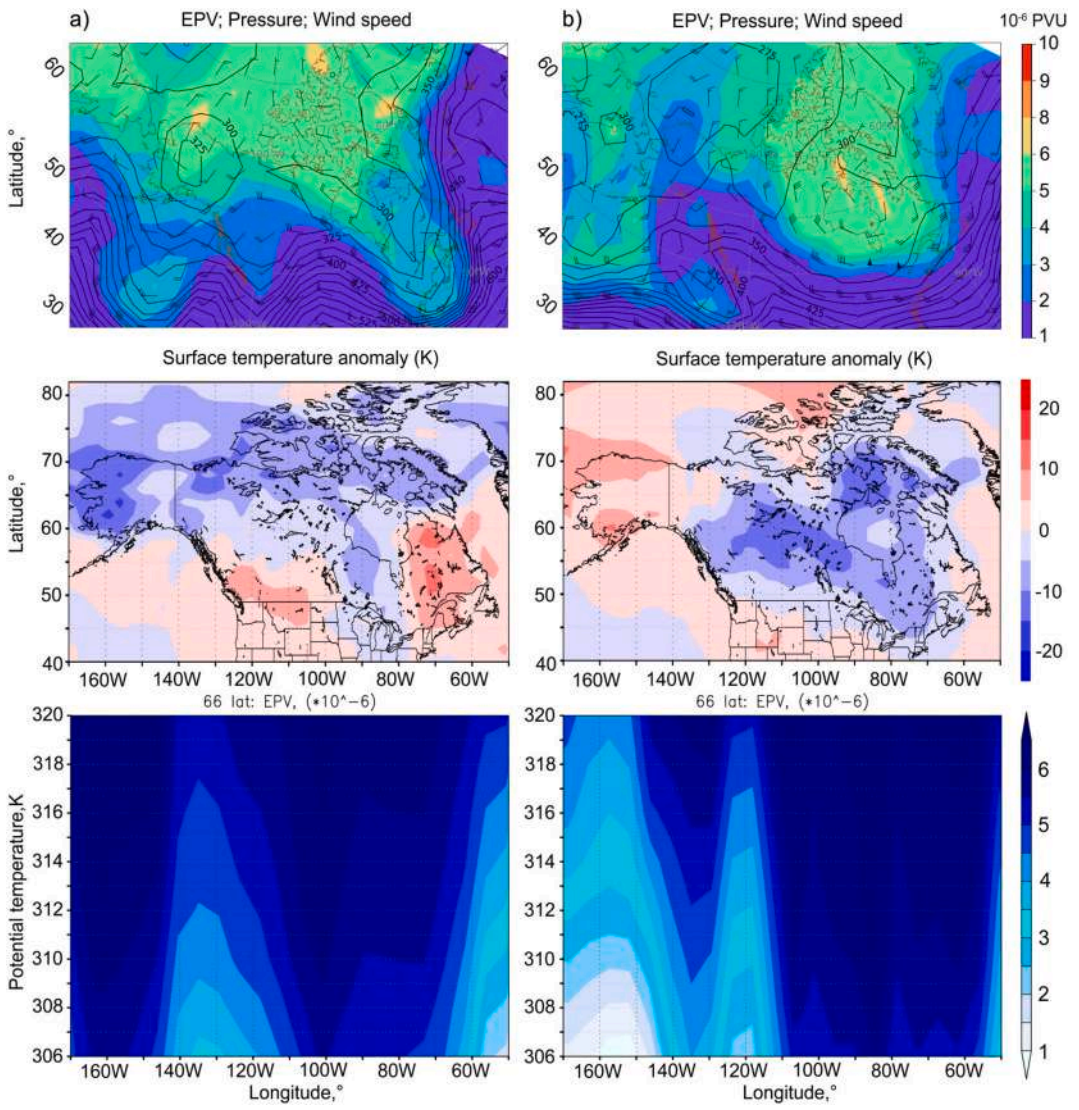

Fig. 11. Ertel's potential vortex, pressure and wind on the 310 K isentropic surface (upper row); daily surface temperature anomaly (middle row), both, for the region 60°W-170°W and 40°N-90°N; vertical cross-section of the Ertel vortex field at 60°W-170°W, 66°N (bottom) on January 10st and 17rd (a, b, respectively).

types is planned for the future study.

CRediT authorship contribution statement

O.N. Toptunova: Writing – original draft, Conceptualization. **M.A. Motsakov:** Software, Data curation. **A.V. Koval:** Supervision, Investigation, Validation. **T.S. Ermakova:** Methodology, Visualization, Editing. **K.A. Didenko:** Formal analysis, Data curation.

Declaration of competing interest

The authors declare that they have no known competing financial interests or personal relationships that could have appeared to influence the work reported in this paper.

Acknowledgements

Temperature, pressure anomalies, wave activity flux analysis, statistical processing, correlation analysis were supported by the Russian Science Foundation (grant #20-77-10006-P), analysis of vertical dynamic coupling, including potential vorticity calculation, was supported by the Russian Science Foundation (grant #24-17-00230).

Data availability

Data will be made available on request.

References

Akritidis, D., Pozzer, A., Zanis, P., Tyrlis, E., Škerlak, B., Sprenger, M., Lelieveld, J., 2016. On the role of tropopause folds in summertime tropospheric ozone over the eastern Mediterranean and the Middle East. Atmos. Chem. Phys. 16, 14025–14039. https://doi.org/10.5194/acp-16-14025-2016.

Anstey, J.A., Osprey, S.M., Alexander, J., Baldwin, M.P., Butchart, N., Gray, L., Kawatani, Y., Newman, P.A., Richter, J.H., 2022. Impacts, processes and projections of the quasi-biennial oscillation. Nat. Rev. Earth Environ. 3, 588–603. https://doi.org/10.1038/s43017-022-00323-7.

Ayarzaguena, B., Charlton-Perez, A., Butler, A., Hitchcock, P., Simpson, I., Polvani, L., Butchart, N., Gerber, E., Gray, L., Hassler, B., Lin, P., Lott, F., Manzini, E., Mizuta, R., Orbe, C., Osprey, S., Saint-Martin, D., Sigmond, M., Taguchi, M., Volodin, E., Watanabe, S., 2020. Uncertainty in the response of sudden stratospheric warmings and stratosphere-troposphere coupling to quadrupled CO2 concentrations in CMIP6 models. J. Geophys. Res. Atmos. 125, e2019JD032345. https://doi.org/10.1029/2019JD032345.

Baldwin, M.P., et al., 2019. 100 years of Progress in Understanding the Stratosphere and Mesosphere. Meteorol. Monogr. 59. https://doi.org/10.1175/AMSMONOGRAPHS-D-19-0003.1, 27.1–27.62.

Baldwin, M.P., Ayarzagüena, B., Birner, T., Butchart, N., Butler, A.H., Charlton-Perez, A. J., Domeisen, D.I.V., Garfinkel, C.I., Garny, H., Gerber, E.P., Hegglin, M.I., Langematz, U., Pedatella, N.M., 2021. Sudden stratospheric warmings. Rev. Geophys. 59, e2020RG000708. https://doi.org/10.1029/2020RG000708.

Baldwin, M.P., Birner, T., Ayarzagüena, B., 2024. Tropospheric amplification of stratosphere–troposphere coupling. Q. J. R. Meteorol. Soc. 1–18. https://doi.org/10.1002/qj.4864.
Butler, A., Charlton-Perez, A., Domeisen, D.I.V., Garfinkel, Ch., Gerber, E.P., Hitchcock, P., Karpechko, A.Yu., Maycock, A.C., Sigmond, M., Simpson, I., Son, S.W., 2019. Sub-seasonal predictability and the stratosphere. In: Robertson, A.W., Vitart, F. (Eds.), Sub-Seasonal to Seasonal Prediction. Elsevier, pp. 223–241. https://doi.org/10.1016/B978-0-12-811714-9.00011-5.
Butler, A.H., Lawrence, Z.D., Lee, S.H., Lillo, S.P., Long, C.S., 2020. Differences between the 2018 and 2019 stratospheric polar vortex split events. Q. J. R. Meteorol. Soc. 146, 3503–3521. https://doi.org/10.1002/qj.3858.
Charlton, A.J., Polvani, L.M., 2007. A new look at stratospheric sudden warmings. Part I: Climatology and modeling benchmarks. J. Clim. 20, 449–469. https://doi.org/10.1175/JCLI3996.1.
Curry, J., 1987. The contribution of radiative cooling to the formation of cold-core anticyclones. J. Atmos. Sci. 44 (18), 2575–2592. https://doi.org/10.1175/1520-0469(1987)044.
Davini, P., Cagnazzo, C., Anstey, J.A., 2014. A blocking view of the stratosphere-troposphere coupling. J. Geophys. Res. 119, 11100–11115. https://doi.org/10.1002/2014JD021703.
Didenko, K.A., Koval, A.V., Ermakova, T.S., 2023. Investigation of stationary planetary waves interactions at different stages of SSW using reanalysis data. Proc. of SPIE, 29th International Symposium on Atmospheric and Ocean Optics. Atmos. Phys. 12780. https://doi.org/10.1117/12.2690456, 1278079–1.
Didenko, K.A., Ermakova, T.S., Koval, A.V., Savenkova, E.N., 2024. Trends of the vertical component of the wave activity flux in the Northern Hemisphere. Geomagn. Aeron. 64 (5), 691–700. https://doi.org/10.1134/S0016793224600632.
Ding, X., Chen, G., Zhang, P., Domeisen, D.I.V., Orbe, C., 2023. Extreme stratospheric wave activity as harbingers of cold events over North America. Commun. Earth Environ. 4, 187. https://doi.org/10.1038/s43247-023-00845-y.
Domeisen, D.I.V., Sun, L., Chen, G., 2013. The role of synoptic eddies in the tropospheric response to stratospheric variability. Geophys. Res. Lett. 40, 4933–4937. https://doi.org/10.1002/grl.50943.
Garfinkel, C.I., Waugh, D.W., Gerber, E.P., 2013. The effect of tropospheric jet latitude on coupling between the stratospheric polar vortex and the troposphere. J. Clim. 26 (6), 2077–2095. https://doi.org/10.1175/JCLI-D-12-00301.1.
Garfinkel, C.I., Son, S.W., Song, K., Aquila, V., Oman, L.D., 2017. Stratospheric variability contributed to and sustained the recent hiatus in Eurasian winter warming. Geophys. Res. Lett. 44, 374–382. https://doi.org/10.1002/2016GL072035.
Gečaitė, I., 2021. Climatology of three-dimensional Eliassen–palm wave activity fluxes in the northern hemisphere stratosphere from 1981 to 2020. Climate 9, 124. https://doi.org/10.3390/cli9080124.
Gelaro, R., McCarty, W., Suárez, Max J., Todling, R., Molod, A., Takacs, L., Randles, C., Darmenov, A., Bosilovich, et al., 2017. The modern-era retrospective analysis for research and applications, Version 2 (MERRA-2). J. Clim. 30 (13), 5419–5454. https://doi.org/10.1175/JCLI-D-16-0758.1.
Gerber, E.P., Orbe, C., Polvani, L.M., 2009. Stratospheric influence on the tropospheric circulation revealed by idealized ensemble forecasts. Geophys. Res. Lett. 36, L24801. https://doi.org/10.1029/2009GL040913.
Hitchcock, P., Simpson, I.R., 2014. The downward influence of stratospheric sudden warmings. J. Atmos. Sci. 71 (10), 3856–3876. https://doi.org/10.1175/JAS-D-14-0012.1.
Hoerling, M.P., Schaack, T.K., Lenzen, A.J., 1991. Global objective tropopause analysis. Mon. Weather Rev. 119, 1816–1831.
Holton, J.R., Tan, H.C., 1980. The influence of the equatorial quasibiennial oscillation on the global circulation at 50 mb. J. Atmos. Sci. 37, 2200–2208.
Holton, J.R., Haynes, P.H., McIntyre, M.E., Douglass, A.R., Rood, R.B., Pfister, L., 1995. Stratosphere-troposphere exchange. Rev. Geophys. 33, 403–440.
Hoskins, B.J., McIntyre, M.E., Robertson, A.W., 1985. On the use and significance of isentropic potential vorticity maps. Q. J. R. Meteorol. Soc. 111 (470), 877–946. https://doi.org/10.1002/qj.49711147002.
Huang, J., Hitchcock, P., Maycock, A.C., McKenna, C.M., Tian, W., 2021. Northern hemisphere cold air outbreaks are more likely to be severe during weak polar vortex conditions. Commun. Earth Environ. 2, 1–11. https://doi.org/10.1038/s43247-021-00215-6.
Karpechko, A.Y., Hitchcock, P., Peters, D.H.W., Schneidereit, A., 2017. Predictability of downward propagation of major sudden stratospheric warmings. Q. J. R. Meteorol. Soc. 143, 1459–1470. https://doi.org/10.1002/qj.3017.
Kidston, J., Scaife, A.A., Hardiman, S.C., Mitchell, D.M., Butchart, N., Baldwin, M.P., Gray, L.J., 2015. Stratospheric influence on tropospheric jet streams, storm tracks and surface weather. Nat. Geosci. 8, 433–440. https://doi.org/10.1038/ngeo2424.
Kolstad, E., Breiteig, T., Scaife, A., 2010. The association between stratospheric weak polar vortex events and cold air outbreaks in the Northern Hemisphere. Q. J. R. Meteorol. Soc. 136, 886–893. https://doi.org/10.1002/qj.620.
Kozubek, M., Lastovicka, J., Krizan, P., 2020. Comparison of key characteristics of remarkable SSW events in the Southern and Northern Hemisphere. Atmosphere 11 (10), 1063. https://doi.org/10.3390/atmos11101063.
Kretschmer, M., Coumou, D., Agel, L., Barlow, M., Tziperman, E., Cohen, J., 2018. More-persistent weak stratospheric polar vortex states linked to cold extremes. Bull. Am. Meteorol. Soc. 99, 49–60. https://doi.org/10.1175/BAMS-D-16-0259.1.
Kunz, A., Konopka, P., Müller, R., Pan, L.L., 2011. Dynamical tropopause based on isentropic potential vorticity gradients. J. Geophys. Res. 116, D01110. https://doi.org/10.1029/2010JD014343.
Lee, S.H., Butler, A.H., 2020. The 2018–2019 Arctic polar vortex. Weather 75, 52–57. https://doi.org/10.1002/wea.3643.
Lehtonen, I., Karpechko, A.Yu., 2016. Observed and modeled tropospheric cold anomalies associated with sudden stratospheric warmings. J. Geophys. Res. Atmos. 121, 1591–1610. https://doi.org/10.1002/2015JD023860.
Mitchell, D.M., Gray, L.J., Anstey, J., Baldwin, M.P., Charlton-Perez, A.J., 2013. The influence of stratospheric vortex displacements and splits on surface climate. J. Climatol. 26, 2668–2682. https://doi.org/10.1175/JCLI-D-12-00030.1.
Moore, J.T., 1993. Isentropic Analysis and Interpretation: Operational Applications to Synoptic and Mesoscale Forecast Problems. National Weather Service Training Center, Kansas City, Missouri, p. 99.
Nishii, K., Nakamura, H., 2005. Upward and downward injection of Rossby wave activity across the tropopause: A new aspect of the troposphere-stratosphere dynamical linkage. Q. J. R. Meteorol. Soc. 131, 545–564. https://doi.org/10.1256/qj.03.91.
Perlwitz, J., Harnik, N., 2004. Downward Coupling between the Stratosphere and Troposphere: the Relative Roles of Wave and Zonal mean Processes. J. Clim. 17, 4902–4909. https://doi.org/10.1175/JCLI-3247.1.
Plumb, R.A., 1985. On the three-dimensional propagation of stationary waves. J. Atmos. Sci. 42 (3), 217–229. https://doi.org/10.1175/1520-0469(1985)042<0217:OTTDPO>2.0.CO;2.
Pogoreltsev, A.I., Aniskina, O.G., Kanukhina, A.Y., Ermakova, T.S., Ugryumov, A.I., Efimova, Y.V., 2020. Tropospheric circulation response to sudden stratospheric warming observed in January 2013. Gidrometeorologiya i Ekologiya. Hydrometeorol. Ecol. (Proceed. Russian State Hydrometeorol. University). 60, 241–254 (In Russian). 10.33933/2074-2762-2020-60-241-254.
Rao, J., Garfinkel, C.I., White, I.P., 2020. Predicting the downward and surface influence of the February 2018 and January 2019 sudden stratospheric warming events in subseasonal to seasonal (S2S) models. J. Geophys. Res. 125, e2019JD031919. https://doi.org/10.1029/2019JD031919.
Savenkova, E.N., Gavrilov, N.M., Pogoreltsev, A.I., 2017. On statistical irregularity of stratospheric warming occurrence during northern winters. J. Atmos. Sol.-Terr. Phy. 163, 14–22. https://doi.org/10.1016/j.jastp.2017.06.007.
Simpson, I.R., Blackburn, M., Haigh, J.D., 2009. The role of eddies in driving the tropospheric response to stratospheric heating perturbations. J. Atmos. Sci. 66 (5), 1347–1365. https://doi.org/10.1175/2008JAS2758.1.
Škerlak, B., Sprenger, M., Pfahl, S., Tyrlis, E., Wernli, H., 2015. Tropopause folds in ERA-Interim: global climatology and relation to extreme weather events. J. Geophys. Res. Atmos. 120, 4860–4877. https://doi.org/10.1002/2014JD022787.
Smith, K.L., Scott, R.K., 2016. The role of planetary waves in the tropospheric jet response to stratospheric cooling. Geophys. Res. Lett. 43, 2904–2911. https://doi.org/10.1002/2016GL067849.
Thompson, D.W.J., Baldwin, M.P., Wallace, J.M., 2002. Stratospheric connection to Northern Hemisphere winter-time weather: implications for prediction. J. Clim. 15, 1421–1428. https://doi.org/10.1175/1520-0442(2002)015,1421:SCTNHW.2.0.CO;2.
Tian, W.S., Huang, J.L., Zhang, J.K., Xie, F., Wang, W.K., Peng, Y.F., 2023. Role of stratospheric processes in climate change: advances and challenges. Adv. Atmos. Sci. 40 (8), 1379–1400. https://doi.org/10.1007/s00376-023-2341-1.
Tomassini, L., Gerber, E.P., Baldwin, M.P., Bunzel, F., Giorgetta, M.J., 2012. The role of stratosphere–troposphere coupling in the occurrence of extreme winter cold spells over northern Europe. J. Adv. Model. Earth Syst. 4, M00A03. https://doi.org/10.1029/2012MS000177.
Vargin, P.N., Volodin, E.M., Karpechko, A.Yu., Pogorel'tsev, A.I., 2015. Stratosphere–troposphere interactions. Her. Russ. Acad. Sci. 85 (1), 56–63. https://doi.org/10.1134/S1019331615010074.
Vargin, P.N., Lukyanov, A.N., Kiryushov, B.M., 2020. Dynamical processes of Arctic stratosphere in the winter 2018-2019. Russ. Meteorol. Hydrol. 46 (6), 387–397. https://doi.org/10.3103/S1068373920060011.
Vargin, P.N., Koval, A.V., Guryanov, V.V., 2022. Arctic Stratosphere Dynamical Processes in the Winter 2021–2022. Atmosphere 13, 1550. https://doi.org/10.3390/atmos13101550.
Vil'fand, R.M., Martazinova, V.F., Tsepelev, V.Y., et al., 2017. Integration of synoptic and hydrodynamic monthly air temperature forecasts. Russ. Meteorol. Hydrol. 42, 485–493. https://doi.org/10.3103/S1068373917080015.
Vitart, F., Anderson, D., 2012. Subseasonal to Seasonal Prediction Project: bridging the gap between weather and climate. WMO 433 Bull. 61, 23–28.
Wei, K., Ma, J., Chen, W., Vargin, P., 2021. Longitudinal peculiarities of planetary waves-zonal flow interactions and their role in stratosphere-troposphere dynamical coupling. Clim. Dyn. 57, 2843–2862. https://doi.org/10.1007/s00382-021-05842-5.
White, I., Garfinkel, C.I., Gerber, E.P., Jucker, M., Aquila, V., Oman, L.D., 2019. The downward influence of sudden stratospheric warmings: association with tropospheric precursors. J. Clim. 32, 85–108. https://doi.org/10.1175/JCLI-D-18-0053.1.
WMO, 1986. Atmospheric Ozone 1985: Global Ozone Research and Monitoring Report. World Meteorological Organization (WMO), Geneva, Switzerland, p. 392.
Woiwode, W., Dörnbrack, A., Bramberger, M., Friedl-Vallon, F., Haenel, F., Höpfner, M., Johansson, S., Kretschmer, E., Krisch, I., Latzko, T., Oelhaf, H., Orphal, J., Preusse, P., Sinnhuber, B.-M., Ungermann, J., 2018. Mesoscale fine structure of a tropopause fold over mountains. Atmos. Chem. Phys. 18, 15643–15667. https://doi.org/10.5194/acp-18-15643-2018.
Xu, F., Liang, X.S., 2020. The synchronization between the zonal jet stream and temperature anomalies leads to an extremely freezing North America in January

2019. Geophys. Res. Lett. 47, e2020GL089689. https://doi.org/10.1029/2020GL089689.
Zhang, Y., Si, D., Ding, Y., Jiang, D., Li, Q., Wang, G., 2022. Influence of major Stratospheric Sudden warming on the unprecedented cold wave in East Asia in January 2021. Adv. Atmos. Sci. 39 (4), 576–590. https://doi.org/10.1007/s00376-022-1318-9.
Zyulyaeva, Yu.A., Zhadin, E.A., 2009. Analysis of three-dimensional Eliassen-Palm fluxes in the lower stratosphere. Russ. Meteorol. Hydrol. 34 (8), 483–490. https://doi.org/10.3103/S1068373909080019.